

Enhanced stochastic oscillations in autocatalytic reactions

Thierry Dauxois

Laboratoire de Physique, Ecole Normale Supérieure Lyon, CNRS, France

Francesca Di Patti

CSDC Centro Interdipartimentale per lo Studio di Dinamiche Complesse, University of Florence, Italy and INFN

Duccio Fanelli

*Dipartimento di Energetica, University of Florence,
Via S. Marta 3, 50139 Florence, Italy and INFN*

Alan J. McKane

*Theoretical Physics, School of Physics and Astronomy,
University of Manchester, Manchester M13 9PL, United Kingdom*

We study a simplified scheme of k coupled autocatalytic reactions, previously introduced by Togashi and Kaneko. The role of stochastic fluctuations is elucidated through the use of the van Kampen system-size expansion and the results compared with direct stochastic simulations. Regular temporal oscillations are predicted to occur for the concentration of the various chemical constituents, with an enhanced amplitude resulting from a resonance which is induced by the intrinsic graininess of the system. The associated power spectra are determined and have a different form depending on the number of chemical constituents, k . We make detailed comparisons in the two cases $k = 4$ and $k = 8$. Agreement between the theoretical and numerical results for the power spectrum are good in both cases. The resulting spectrum is especially interesting in the $k = 8$ system, since it has two peaks, which the system-size expansion is still able to reproduce accurately.

PACS numbers: 02.50.Ey, 05.40.-a, 82.20.Uv

I. INTRODUCTION

Autocatalytic reactions have long fascinated physicists and chemists because of their unique features [1]. A chemical reaction is called autocatalytic if one of the reaction products is itself a catalyst for the chemical reaction. Part of the reason for the interest in these types of reactions stems from the fact that even if only a small amount of the catalyst is present, the reaction may start off slowly, but will quickly speed up once more catalyst is produced. If the reactant is not replaced, the process will again slow down producing the typical sigmoid shape for the concentration of the product. All this is for a single chemical reaction, but of greater interest is the case of many chemical reactions, where one or more reactions produce a catalyst for some of the other reactions. Then the whole collection of constituents is called an autocatalytic set [2]. In addition to the interesting properties of autocatalytic sets, there is also an intriguing possibility that “bootstrap” reactions such as this may have had an important role in producing complex or self-replicating molecules required for the origin of life on Earth [3, 4, 5, 6].

Theoretical studies of the properties of autocatalytic reactions are typically of two kinds. In the first, rate equations for the reactions are written down and these are either solved numerically or their properties investigated using the techniques used in the study of dynamical systems. An alternative is to carry out computer simulations of the actual reactions themselves. However

there is a third possibility: using methods from the theory of stochastic processes an analytic approach to the full model (and not just the mean field version) is possible. In the last few years this last approach has been used for systems which are closely related to autocatalytic reactions, such as predator-prey interactions [7], metabolic reactions [8], and epidemic models [9]. These all show oscillatory behavior in the number of individuals or constituents, which arise from feedbacks. These oscillations are distinct from the limit cycles found in the rate equations, and are purely stochastic in origin. The main tool that is used to analyze these systems is the system-size expansion of van Kampen [10, 11] which gives very good agreement with the simulation results, even for systems of a moderate size.

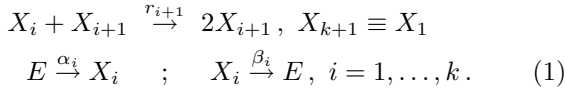
In this paper we apply this technique to the autocatalytic reaction scheme studied by Togashi and Kaneko [12, 13]. In most autocatalytic reactions there are two types of constituent: the autocatalytic and the substrate. The number of the latter type are kept constant by continually feeding them in, however the former are not injected nor extracted from the system. In this sense the system is closed as far as the autocatalytic constituents are concerned, but open for the substrate. In the scheme that Togashi and Kaneko investigate, the reactions are cyclic, with k constituents X_1, \dots, X_k reacting according to $X_i + X_{i+1} \rightarrow 2X_{i+1}$ with $X_{k+1} \equiv X_1$, $i = 1, \dots, k$. The chemicals are assumed to be in a container which is well-stirred, but with the possibility of diffusing across the surface of the container into a particle reservoir.

In their approach Togashi and Kaneko [12, 13] use only computer simulation to study this reaction scheme. The analytic techniques we will use begin by writing down the master equation for their reaction scheme, and then studying it through a systematic expansion in $N^{-1/2}$, where N is the system size. To leading order one finds the rate equations which appear in [12], and to next-to-leading order a Langevin equation which describes the fluctuations about the stable fixed point of the rate equations. From previous work we expect that (i) this first-order correction will be sufficient to yield results which are in good agreement with simulation data, (ii) the large amplitude of the oscillations can be understood as a resonant effect. One of the strengths of the technique is that the next-to-leading order corrections give *linear* Langevin equations which can be analyzed exactly for arbitrary values of k .

The outline of the paper is as follows. In Section II we derive the equations which govern the dynamics of the system, both in the deterministic limit and for the fluctuations about this limit. These fluctuations are analyzed in Section III by calculating the power spectra for each chemical species i . Theoretical predictions are then compared to direct simulations for the case $k = 4$ and $k = 8$. Finally in Section IV we sum up and discuss possible future work. An Appendix contains the intermediate steps required to find the equations given in the main text.

II. GOVERNING EQUATIONS

The autocatalytic reaction scheme described in Section I can be formulated as



Here r_i, α_i and β_i (with $r_{k+1} \equiv r_1$), are the rates at which the reactions take place and E is the null constituent. Such constituents have to be included so that the number of molecules of type X_i, n_i , are all independent. If the size of the system is denoted by N , then $\sum_{i=1}^k n_i + n_E = N$, where n_E is the number of null constituents. While N is fixed, n_E may vary as the total number of molecules changes with time. In practice, n_E does not explicitly appear in the formalism; it is always replaced by $N - \sum_{i=1}^k n_i$. The rate constants α_i and β_i in Eq. (1) represent the interactions of the system with the particle reservoir outside the container. In effect α_i and β_i are the rate at which molecules appear and disappear from the system, and thus are analogous to birth and death rates.

As an aside, we note that reaction rates which result from a binary encounter should be scaled by the volume of the system, V . That is, $r_i \rightarrow r_i/V$. This follows from a straightforward kinetic theory argument [14]. This

is an innocent modification as far as this study is concerned, since it is carried out at constant volume, but it becomes crucially important when the volume is allowed to change, as it does in the analysis of the phase transition reported in [12, 13].

The state of the system is labeled by the set of integers $\{n_1, \dots, n_k\}$ and, under the assumption that the transitions from this state to any other only depends on these integers, the system is Markov and may be described in terms of a master equation. In constructing the master equation we need to give the transition rates $T(\mathbf{n}'|\mathbf{n})$ from the state \mathbf{n} to the state \mathbf{n}' , where $\mathbf{n} \equiv (n_1, \dots, n_k)$. If the system is well-stirred, so that the probability of a reaction taking place is proportional to its rate and the number of reactant molecules, then from Eq. (1) these transition rates are

$$\begin{aligned} T(n_1, \dots, n_i - 1, n_{i+1} + 1, \dots, n_k | \mathbf{n}) &= r_{i+1} \frac{n_i}{N} \frac{n_{i+1}}{N}, \\ T(n_1, \dots, n_i + 1, \dots, n_k | \mathbf{n}) &= \alpha_i \left(1 - \frac{\sum_{j=1}^k n_j}{N} \right), \\ T(n_1, \dots, n_i - 1, \dots, n_k | \mathbf{n}) &= \beta_i \frac{n_i}{N}. \end{aligned} \quad (2)$$

The master equation for the probability that the system is in state \mathbf{n} at time t , $P(\mathbf{n}, t)$, may now be written down:

$$\begin{aligned} \frac{dP(\mathbf{n}, t)}{dt} &= \sum_{i=1}^k (\mathcal{E}_i \mathcal{E}_{i+1}^{-1} - 1) \\ &\times [T(n_1, \dots, n_i - 1, n_{i+1} + 1, \dots, n_k | \mathbf{n}) P(\mathbf{n}, t)] \\ &+ \sum_{i=1}^k (\mathcal{E}_i^{-1} - 1) [T(n_1, \dots, n_i + 1, \dots, n_k | \mathbf{n}) P(\mathbf{n}, t)] \\ &+ \sum_{i=1}^k (\mathcal{E}_i - 1) [T(n_1, \dots, n_i - 1, \dots, n_k | \mathbf{n}) P(\mathbf{n}, t)] \end{aligned} \quad (3)$$

where $\mathcal{E}_i^{\pm 1}$ are the step-operators introduced by van Kampen [10]:

$$\mathcal{E}_i^{\pm 1} f(\mathbf{n}) = f(n_1, \dots, n_i \pm 1, \dots, n_k). \quad (4)$$

Equations such as (3) are difficult to analyze, but if one is particularly interested in large or moderately sized values of N , then the system-size expansion provides an elegant way of encapsulating the essential aspects of the model. The key assumption of the method is to write [10]

$$\frac{n_i}{N} = \phi_i(t) + \frac{\xi_i(t)}{\sqrt{N}}. \quad (5)$$

From this relation, $\lim_{N \rightarrow \infty} (n_i/N) = \phi_i(t)$, the fraction of the molecules which are of type X_i at time t , within the mean-field ($N \rightarrow \infty$) limit. The fluctuations about these are assumed to be Gaussian, hence the $1/\sqrt{N}$ in Eq. (5). One of the consequences of this assumption is that one is looking at a regime sufficiently far from boundaries that

the probability density functions of the X_i are Gaussian. This implies that stochastic extinctions will not be well-described by the method, at least to leading order.

Substituting Eq. (5) into Eq. (3) allows us to expand the master equation as a power series in $1/\sqrt{N}$. To see this we first note that the step operators (4) take a particularly simple form within the method [10]

$$\mathcal{E}_i^{\pm 1} = 1 \pm \frac{1}{\sqrt{N}} \frac{\partial}{\partial \xi_i} + \frac{1}{2N} \frac{\partial^2}{\partial \xi_i^2} + \dots \quad (6)$$

If we set $P(\mathbf{n}, t)$ equal to $\Pi(\boldsymbol{\xi}, t)$, the left-hand side of the master equation becomes [10]

$$\frac{dP(\mathbf{n}, t)}{dt} = \frac{\partial \Pi(\boldsymbol{\xi}, t)}{\partial t} - \sqrt{N} \sum_{i=1}^k \frac{\partial \Pi(\boldsymbol{\xi}, t)}{\partial \xi_i} \frac{d\phi_i}{dt}. \quad (7)$$

Substituting Eq. (5) into the right-hand side of the master equation (3), and using the transition rates (2), we may equate terms of the same order in $1/\sqrt{N}$ on the left- and right-hand sides. To leading order this gives (see Appendix A for details)

$$\frac{d\phi_i}{d\tau} = (r_i \phi_{i-1} - r_{i+1} \phi_{i+1}) \phi_i + \alpha_i \left(1 - \sum_{j=1}^k \phi_j \right) - \beta_i \phi_i, \quad (8)$$

where τ is a rescaled time: $\tau = t/N$. At next order one finds a Langevin equation:

$$\frac{d\xi_i}{d\tau} = \sum_{j=1}^k M_{ij} \xi_j(\tau) + \eta_i(\tau), \quad (9)$$

where M is a $k \times k$ matrix which can be found from Eqs. (A5) and (A7), and η_i is a Gaussian white noise with zero mean and correlator

$$\langle \eta_i(\tau) \eta_j(\tau') \rangle = B_{ij} \delta(\tau - \tau'), \quad (10)$$

and B_{ij} is another $k \times k$ matrix given by Eq. (A6).

The first equation, Eq. (8), is a deterministic equation for the fraction of molecules which are of type i . It agrees with that of Togashi and Kaneko [12], if one takes into account that their equations are for concentrations and so contain the (constant) concentrations of the species in the reservoir. There is also an additional term $\sum_j \phi_j$ in Eq. (8), which is typically present when mean-field equations are derived in systems with a fixed size, but not in the phenomenologically postulated form. For small concentrations it will not be important, but clearly it will have an effect as the ceiling on particle numbers is felt, reducing the number of molecules entering the container from the reservoir, as it should. The second equation, Eq. (9), is a stochastic differential equation for the deviation from these mean-field values. It is the analysis of these two equations that allow us to describe the stochastic aspects of the autocatalytic reactions in a quantitative way.

III. ANALYSIS OF THE FLUCTUATIONS

In their numerical studies, Togashi and Kaneko [12, 13] looked at the simplest case of the model where the rates r_i, α_i and β_i were the same for all chemical species. To illustrate our method we will do the same, and so from now on we will drop the subscript i on these constants, but it should be clear that our analysis also applies to the general situation where they are different for each species. With this choice, the deterministic equations (8) have a single fixed point:

$$\phi^* = \frac{\alpha}{\beta + k\alpha}, \quad (11)$$

where the asterisk denotes the fixed point value.

If N is so large that the fluctuations are completely negligible, then the system tends towards a state where the fractions of the chemical species in the system are equal, and given by Eq. (11), and stays there. Of course, if N is finite this is no longer the case and there are fluctuations about this stationary state — and as we will see these can be significant even if N is quite large. Since these fluctuations are expected to be oscillatory, we begin their analysis by taking the Fourier transform of Eq. (9) to find

$$\sum_{j=1}^k (-i\omega \delta_{ij} - M_{ij}) \tilde{\xi}_j(\omega) = \tilde{\eta}_i(\omega), \quad (12)$$

where the \tilde{f} denotes the Fourier transform of the function f . Defining the matrix $-i\omega \delta_{ij} - M_{ij}$ to be $\Phi_{ij}(\omega)$, the solution to Eq. (12) is

$$\tilde{\xi}_i(\omega) = \sum_{j=1}^k \Phi_{ij}^{-1}(\omega) \tilde{\eta}_j(\omega). \quad (13)$$

To identify the dominant frequency of the oscillatory behavior, we compute the power spectrum for the i th species, $P_i(\omega)$, from Eq. (13):

$$P_i(\omega) \equiv \langle |\tilde{\xi}_i(\omega)|^2 \rangle = \sum_{j=1}^k \sum_{l=1}^k \Phi_{ij}^{-1}(\omega) B_{jl} (\Phi^\dagger)^{-1}_{li}(\omega), \quad (14)$$

Since $\Phi = -i\omega I - M$, where I is the $k \times k$ unit matrix, and since M and B are independent of ω , the structure of $P_i(\omega)$ is that of a polynomial of order $2k$ divided by another polynomial of degree $2k$. The explicit form of the denominator is $|\det \Phi(\omega)|^2$.

From previous investigations of fluctuations of a similar kind [7, 8, 9], we expect that the fluctuations about the stationary state (11) will be enhanced by a resonant effect: for values of ω for which $|\det \Phi(\omega)|$ is a minimum, the power spectra will show peaks which correspond to larger than expected fluctuations at that frequency. This effect was first conjectured by Bartlett [15] in the context of the modeling of measles epidemics, and later elaborated upon by Nisbet and Gurney [16], who called these

stochastically induced cycles, quasi-cycles. However it is only in the last few years that explicit calculations within the system-size expansion have been carried out and a quantitative understanding of the phenomenon has emerged [7].

To understand the analytic structure of the power spectra, we begin by supposing that we can neglect the effects of the numerator on the right-hand side of Eq. (14), and simply determine the dominant frequency by looking for the value which minimizes $|\det \Phi(\omega)|$. The effect of the numerator will be to shift this frequency; we are assuming as a first approximation that this shift will be small, as indeed it has been found to be in some cases [7]. If λ_j are the eigenvalues of M , then the denominator of the expression for the power spectra may be written as

$$|\det \Phi(\omega)|^2 = \prod_{j=1}^k (-i\omega - \lambda_j) (i\omega - \lambda_j^*) . \quad (15)$$

Since M is real, the λ_j will be real or come in complex conjugate pairs, so that the products in Eq. (15) has one of two forms:

- (i) If λ is real, the two factors involving this eigenvalue give $(\omega^2 + \lambda^2)$.
- (ii) If λ is complex: $\lambda = \lambda_R + i\lambda_I$, the four terms involving λ and λ^* give

$$|\omega^2 + (\lambda_R^2 - \lambda_I^2) + 2i\lambda_R\lambda_I|^2 . \quad (16)$$

The resonant effect has its origin in the structure of the factor coming from the complex eigenvalues shown in the expression (16). It is smallest, and so gives the largest contribution when it is in the denominator, for frequencies which satisfy

$$\omega_c^2 = \lambda_I^2 - \lambda_R^2 . \quad (17)$$

If there are several pairs of complex eigenvalues and their conjugates, the largest contribution should come from the pair for which $\lambda_R\lambda_I$ is smallest. Clearly this will only be approximately true since, not only are we neglecting the numerator, but also the factors $(\omega^2 + \lambda^2)$ coming from real eigenvalues, as well as those coming from other complex conjugate pairs. However, as we will now see by looking at two specific cases, $k = 4$ and $k = 8$, these approximations appear to be remarkably good.

We study the cases $k = 4$ and $k = 8$ because they are the smallest even values of k for which one complex conjugate pair and two distinct complex conjugate pairs, respectively, exist (there are two complex conjugate pairs for $k = 6$, but they are equal, and three for $k = 8$, but two of these are equal). We therefore expect to see one peak in the power spectra when $k = 4$ and two when $k = 8$. Our analysis, and the accuracy of our approximations, can be directly checked by numerical simulation of the chemical reaction system (1) by use of the Gillespie algorithm [14, 17]. This produces realizations of the

stochastic dynamics which are equivalent to those found from the master equation (3). Averaging over many of these realizations gives us power spectra after Fourier transformation, which are exact to a given numerical accuracy. We now investigate the two cases $k = 4$ and $k = 8$ in more detail.

A. Power spectra when $k = 4$

The time evolution of the species is depicted Figure 1. This clearly displays large oscillations which we aim to investigate analytically. Before beginning this analysis, we observe that species 1, 3 (odd) and 2, 4 (even) are paired together and move up and down from the reference mean-field level in a synchronized fashion. This fact was already recognized in [12, 13] and shown to drive successive switches between the 1-3 or 2-4 rich states, close to the absorbing boundary, i.e. when a small number of molecules is simulated. The rate at which the changes occur is controlled by the diffusion parameter. However, the details of the transitions stem from a purely dynamical effect which cannot be captured within the perturbative analysis developed here.

Let us now turn to analytically characterizing the aforementioned oscillatory regime. To this end we begin by determining the eigenvalues of the M matrix. From Eq. (A14), these are

$$\begin{aligned} \lambda_0 &= \beta + 4\alpha, & \lambda_2 &= \beta, \\ \lambda_1 &= \beta + 2ir\phi^*, & \lambda_3 &= \lambda_1^*. \end{aligned} \quad (18)$$

Within the approximations we have discussed, we would expect that there should be a single peak in the power spectrum for any one of the chemical species at a frequency given by (see Eq. (17))

$$\omega_c^2 = 4r^2 (\phi^*)^2 - \beta^2 = \frac{4r^2 \alpha^2}{(\beta + 4\alpha)^2} - \beta^2 . \quad (19)$$

In Fig. 2 we show the power spectrum (for the chemical species $i = 2$) found by averaging over 500 realizations from the Gillespie algorithm, together with that found from Eq. (14) using the matrices B and M given in the Appendix. The good agreement between the simulation results and those found from applying the system-size expansion, shows that the method works well for $N = 5000$. The parameters used in this case were $r = 10$ and $\alpha = \beta = 1/64$, which gives a value of $\omega_c \approx 4$ from Eq. (19). From Fig. 2 we see this is a surprising good estimate for the position of the peak, given the significant frequency dependence which we have neglected to obtain the estimate (17).

Another check of the accuracy of these approximations, and so of Eq. (17), is to imagine increasing the parameter β at fixed r and α , and asking when ω_c^2 will become zero, and so at what frequency will the peak in the power

spectra disappear. From Eq. (19) we estimate this to be

$$\beta \sim \frac{2r\alpha}{\beta} \text{ or } \beta \sim \sqrt{2r\alpha}, \quad (20)$$

which equals 0.56 for the values of r and α used in Fig. 2. Once again this agrees well with the full spectrum which predicts the peak to disappear at about the same value. As a final check, we measure the position of the peak from a set of simulations run at different values of r . Direct measurements (symbols) are compared to the theory (solid line) in Figure 3 and are in good quantitative agreement. Again, we recall that adjusting the rate r can be equivalently seen as modifying the volume of the system, which is the setting investigated in [12, 13].

B. Power spectra when $k = 8$

From Eq. (A14), the eigenvalues of the M matrix are

$$\begin{aligned} \lambda_0 &= \beta + 8\alpha, & \lambda_4 &= \beta, \\ \lambda_1 &= \beta + \sqrt{2}ir\phi^*, & \lambda_7 &= \lambda_1^*, \\ \lambda_2 &= \beta + 2ir\phi^*, & \lambda_6 &= \lambda_2^*, \\ \lambda_3 &= \beta + \sqrt{2}ir\phi^*, & \lambda_5 &= \lambda_3^*. \end{aligned} \quad (21)$$

Since there are two distinct complex conjugate pairs we would expect to find two peaks in the power spectra, one at $\omega_c^2 = 2r^2(\phi^*)^2 - \beta^2$ and the other at $\omega_c^2 = 4r^2(\phi^*)^2 - \beta^2$. For small β , one peak will be at a frequency $\sqrt{2}$ times the other. We would also expect that the peak at

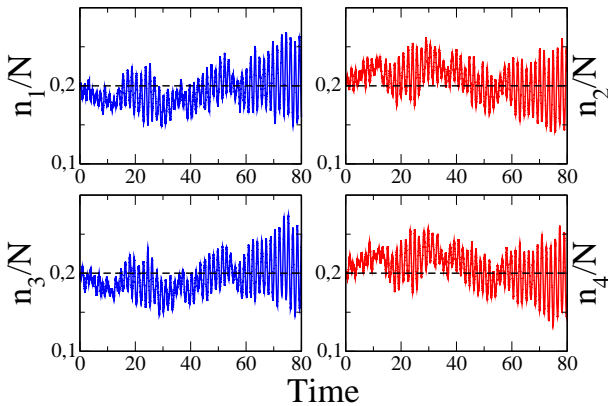


FIG. 1: (Color online) Time evolution of selected species, $i = 1, 2, 3, 4$ in clockwise order for the case $k = 4$. Here $r = 10$, $\alpha = \beta = 1/64$, $N = 8192$. The dashed line indicates the mean field solution. The species display a clear oscillatory trend about their mean field values. A paired synchronization, (1,3) vs. (2,4) rich states, is also visible, as already observed in [12, 13].

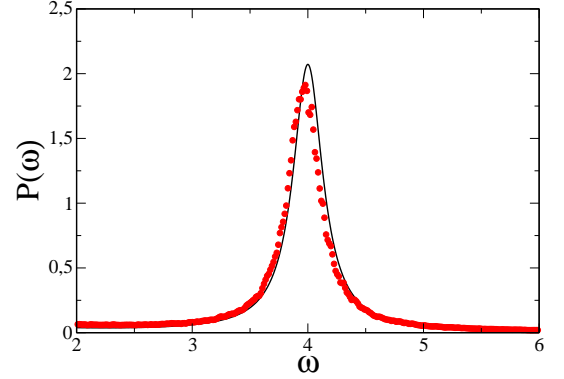


FIG. 2: (Color online) Power spectrum of species $i = 2$ when $k = 4$. The analytical curve is shown as a solid line and the simulation (average over 500 independent realizations) as symbols. Here $r = 10$, $\alpha = \beta = 10/64$, $N = 5000$.

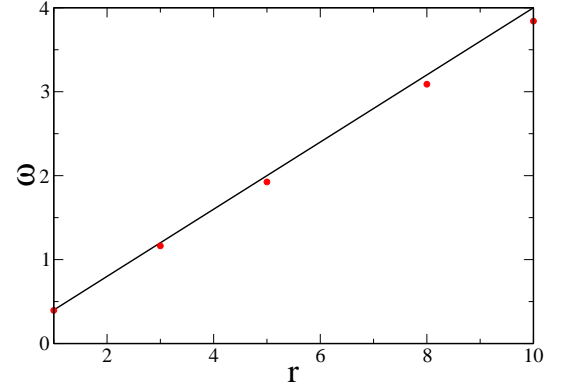


FIG. 3: (Color online) The position of the peak in the power spectrum (for species $i = 2$ when $k = 4$) plotted as function of the rate constant r . Symbols refers to the stochastic simulations, while the solid line shows the analytical prediction. Here $\alpha = \beta = 1/64$, $N = 5000$

lower frequency would be larger than the one at higher frequency, since $\lambda_R \lambda_I$ is smaller for the former. That is, the pole in the power spectra in the complex frequency squared plane is nearer to the real axis for the peak at lower frequency, and so should have a bigger effect. So, in summary, our approximations indicate that the peaks in the power spectra should be given by

$$\omega_{c1}^2 = \frac{2r^2\alpha^2}{(\beta + 8\alpha)^2} - \beta^2, \quad \omega_{c2}^2 = \frac{4r^2\alpha^2}{(\beta + 8\alpha)^2} - \beta^2, \quad (22)$$

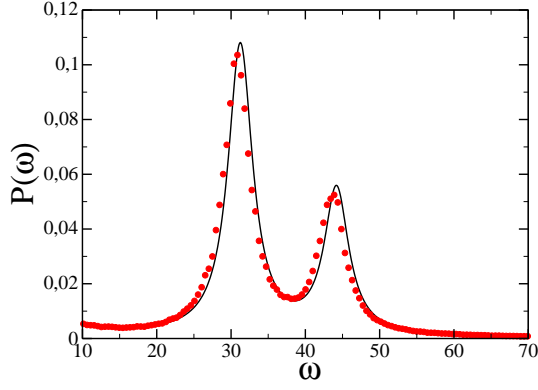


FIG. 4: (Color online) Power spectrum of the time series for species $i = 2$ when $k = 8$. The analytical result (solid line) is superimposed onto the simulations (symbols), averaged over 500 independent realizations. Here $r = 200$, $\alpha = 1.9$, $\beta = 2$, $N = 7000$.

with the peak at $\omega = \omega_{c1}$ larger than the one at $\omega = \omega_{c2}$. The results of plotting the full spectrum found from Eq. (14) and simulation results are shown in Fig. 4 for $r = 200$, $\alpha = 1.9$ and $\beta = 2$. This corresponds to peaks at $\omega = 31.2$ and $\omega = 44.14$, according to Eqs. (22), which once again agrees very well with the results displayed in the figure, as does the prediction that the peak nearest the origin should be the largest.

IV. CONCLUSION

Auto-catalytic networks are central in many different contexts and play an important role in intracellular biochemical reaction schemes. In this latter scenario, species are confined in a closed volume, delimited by the cellular membrane. Low concentration can occasionally develop resulting from the complex mutual interaction between microscopic actors. Under such conditions, fluctuations matter and the effects of the intrinsic discreteness need to be properly accounted for. In other words, continuous kinetic equations prove inadequate, finite size corrections becoming significant. These aspects were numerically substantiated by Togashi and Kaneko [12, 13] within the framework of a simplified system of k coupled autocatalytic reactions.

In this paper we have taken this forward by studying analytically the associated master equation via a systematic expansion in power of $N^{-1/2}$, where N is the system size. To leading order, the mean-field rate equations are recovered, while higher order corrections enable us to explain the large amplitude of the oscillations as detected in direct simulations. Importantly, the calculation applies to arbitrary values of k . For $k = 4$ a peak in the power spectrum is found, while for $k = 8$ two peaks develop. To the best of our knowledge, this is the first time that a double-peaked power spectrum has been predicted to emerge as a resonant effect, within a van Kampen type

of analysis. In both cases, theory and simulations agree well thus confirming the importance of finite N contributions. Possible extensions of the present work include taking spatial variations into account. This could yield spatial oscillations in the species concentration, which would again be driven by the discreteness of the system components.

Acknowledgments

We wish to thank K. Kaneko for useful correspondence. AJM wishes to thank the EPSRC (UK) for financial support under grant GR/T11784/01.

APPENDIX A: THE FINITE N EXPANSION

In this appendix we will give the intermediate steps of the calculation using the system size expansion, starting with the master equation (3) and ending with the results (8)-(10). We will also give the explicit expressions for the matrices M and B .

Applying the ansatz (5) to the right-hand side of Eq. (3), the step-operators (4) take the form (6), the n_i in the transition rates (2) are replaced by ϕ_i and ξ_i using Eq. (5) and $P(\mathbf{n}, t)$ becomes $\Pi(\boldsymbol{\xi}, t)$. This yields the following terms:

- (a) Terms of order $N^{-1/2}$:

$$\sum_{i=1}^k \left\{ r_{i+1} \phi_i \phi_{i+1} \left[\frac{\partial}{\partial \xi_i} - \frac{\partial}{\partial \xi_{i+1}} \right] - \alpha_i \left(1 - \sum_{j=1}^k \phi_j \right) \frac{\partial}{\partial \xi_i} + \beta_i \phi_i \frac{\partial}{\partial \xi_i} \right\} \Pi(\boldsymbol{\xi}, t). \quad (\text{A1})$$

- (b) Terms of order N^{-1} and involving first order derivatives:

$$\sum_{i=1}^k \left\{ r_{i+1} \phi_i \frac{\partial}{\partial \xi_i} \xi_{i+1} + r_{i+1} \phi_{i+1} \frac{\partial}{\partial \xi_i} \xi_i - r_{i+1} \phi_i \frac{\partial}{\partial \xi_{i+1}} \xi_{i+1} - r_{i+1} \phi_{i+1} \frac{\partial}{\partial \xi_{i+1}} \xi_i + \alpha_i \sum_{j=1}^k \frac{\partial}{\partial \xi_i} \xi_j + \beta_i \frac{\partial}{\partial \xi_i} \xi_i \right\} \Pi(\boldsymbol{\xi}, t). \quad (\text{A2})$$

- (c) Terms of order N^{-1} and involving second order derivatives:

$$\frac{1}{2} \sum_{i=1}^k \left\{ r_{i+1} \phi_i \phi_{i+1} \left[\frac{\partial^2}{\partial \xi_i^2} + \frac{\partial^2}{\partial \xi_{i+1}^2} - 2 \frac{\partial^2}{\partial \xi_i \partial \xi_{i+1}} \right] + \alpha_i \left(1 - \sum_{j=1}^k \phi_j \right) \frac{\partial^2}{\partial \xi_i^2} + \beta_i \phi_i \frac{\partial^2}{\partial \xi_i^2} \right\} \Pi(\boldsymbol{\xi}, t). \quad (\text{A3})$$

Introducing $\tau = t/N$, the terms of order $N^{-1/2}$ in Eq. (A1) may be identified with the second term on the right-hand side of Eq. (7). This gives the N deterministic equations (8). The terms of order N^{-1} in Eqs. (A2) and (A3), are now identified with the remaining term on the right-hand side of Eq. (7). This resulting equation is a Fokker-Planck equation:

$$\frac{\partial \Pi}{\partial \tau} = - \sum_i \frac{\partial}{\partial \xi_i} [A_i(\xi) \Pi] + \frac{1}{2} \sum_{i,j} B_{ij} \frac{\partial^2 \Pi}{\partial \xi_i \partial \xi_j}. \quad (\text{A4})$$

From Eq. (A2) we see that the $A_i(\xi)$ are linear functions of the ξ_j and from Eq. (A3) that the B_{ij} are independent of them. Explicitly:

$$A_i(\xi) = (r_i \phi_{i-1} - r_{i+1} \phi_{i+1}) \xi_i + r_i \phi_i \xi_{i-1} - r_{i+1} \phi_i \xi_{i+1} - \alpha_i \sum_{j=1}^k \xi_j - \beta_i \xi_i, \quad (\text{A5})$$

and

$$B_{ij} = \begin{cases} -r_i \phi_{i-1} \phi_i, & \text{if } j = i-1 \\ r_{i+1} \phi_i \phi_{i+1} + r_i \phi_i \phi_{i-1} \\ + \alpha_i \left(1 - \sum_{j=1}^k \phi_j\right) + \beta_i \phi_i, & \text{if } j = i \\ -r_{i+1} \phi_i \phi_{i+1}, & \text{if } j = i+1 \end{cases} \quad (\text{A6})$$

In Eqs. (A5) and (A6), $\phi_{k+1} \equiv \phi_1$ and $\xi_{k+1} \equiv \xi_1$, which follows from the cyclic nature of the model.

Since the $A_i(\xi)$ are linear functions of the ξ_j we may write them as

$$A_i(\xi) = \sum_{j=1}^k M_{ij} \xi_j. \quad (\text{A7})$$

This means that the probability distribution at next-to-leading order, $\Pi(\xi, \tau)$, is completely determined by the two $k \times k$ matrices M and B , whose elements are independent of the ξ_j , and only functions of the ϕ_j . For our purposes, where we need to Fourier analyze the fluctuations, it is more convenient not to use the formulation in which the fluctuations are described by a Fokker-Planck equation, but rather in terms of Langevin equations. The Fokker-Planck equation (A4) is completely equivalent to the Langevin equation (9) with the correlator (10) [18, 19], and it is this formalism that we will use.

In principle the matrices M and B are time dependent, since ϕ_j is. However, in practice we are interested in fluctuations about the stationary state, and so we are only interested in the values that the ϕ_j take on at late times. Furthermore, in Section III we studied the simple case $r_i = r, \alpha_i = \alpha$ and $\beta_i = \beta$, for which the relevant value of the ϕ_j is given by Eq. (11). With these assumptions M and B are given by

$$M = \begin{bmatrix} m_0 & m_1 & m_2 & m_2 & \dots & m_2 & m_3 \\ m_3 & m_0 & m_1 & m_2 & \dots & m_2 & m_2 \\ m_2 & m_3 & m_0 & m_1 & \dots & m_2 & m_2 \\ m_2 & m_2 & m_3 & m_0 & \dots & m_2 & m_2 \\ \dots & \dots & \dots & \dots & \dots & \dots & \dots \\ m_2 & m_2 & m_2 & m_2 & \dots & m_0 & m_1 \\ m_1 & m_2 & m_2 & m_2 & \dots & m_3 & m_0 \end{bmatrix}, \quad (\text{A8})$$

where

$$m_0 = -\alpha - \beta, m_1 = -\alpha - r\phi^*, m_2 = -\alpha, m_3 = -\alpha + r\phi^*, \quad (\text{A9})$$

and

$$B = \begin{bmatrix} b_0 & b_1 & 0 & \dots & 0 & b_1 \\ b_1 & b_0 & b_1 & \dots & 0 & 0 \\ 0 & b_1 & b_0 & \dots & 0 & 0 \\ \dots & \dots & \dots & \dots & \dots & \dots \\ 0 & 0 & 0 & \dots & b_0 & b_1 \\ b_1 & 0 & 0 & \dots & b_1 & b_0 \end{bmatrix}, \quad (\text{A10})$$

where

$$b_0 = 2r(\phi^*)^2 + \beta\phi^* + \alpha(1 - k\phi^*), b_1 = -r(\phi^*)^2. \quad (\text{A11})$$

We note that M is a circulant matrix [20], and therefore its eigenvalues are given by

$$\lambda_\ell = \sum_{j=1}^k m_{1j} e^{2\pi i(j-1)\ell/k}, \quad \ell = 0, 1, \dots, k-1, \quad (\text{A12})$$

where m_{1j} is the element of M in the first row and j th column. In fact, M is not the most general form of circulant matrix; $(k-3)$ entries in each row are equal (to m_2). This leads to a simplified form for the eigenvalues:

$$\begin{aligned} \lambda_\ell &= m_0 + m_1 e^{2\pi i\ell/k} + m_3 e^{-2\pi i\ell/k} + m_2 \sum_{j=2}^{k-2} e^{2\pi i j\ell/k} \\ &= m_0 + m_1 e^{2\pi i\ell/k} + m_3 e^{-2\pi i\ell/k} - m_2 \frac{\sin(3\pi\ell/k)}{\sin(\pi\ell/k)}, \end{aligned} \quad (\text{A13})$$

where in the last line $\ell \neq 0$. Putting in the values from Eq. (A9) gives

$$\lambda_\ell = \begin{cases} \beta + k\alpha, & \text{if } \ell = 0 \\ \beta + 2ir\phi^* \sin(2\pi\ell/k), & \text{if } \ell \neq 0. \end{cases} \quad (\text{A14})$$

-
- [1] P. Gray and S. K. Scott. *J. Phys. Chem.* **89**, 22 (1985).
 - [2] S. Jain and S. Krishna. *Phys. Rev. Lett.* **81**, 5684 (1998).
 - [3] F. Dyson. *Origins of Life* (Cambridge University Press, Cambridge, England, 1985).
 - [4] S. A. Kauffman. *J. Theor. Biol.* **119**, 1 (1986); *The Origins of Order* (Oxford University Press, Oxford, 1993).
 - [5] P. F. Stadler and P. Schuster, *Bull. Math. Biol.* **52**, 484 (1990).
 - [6] G. Wächtershäuser. *Proc. Natl. Acad. Sci. U.S.A.* **87**, 200 (1990).
 - [7] A. J. McKane and T. J. Newman. *Phys. Rev. Lett.* **94**, 218102 (2005).
 - [8] A. J. McKane, J. D. Nagy, T. J. Newman, and M. O. Stefanini. *J. Stat. Phys.* **128**, 165 (2007).
 - [9] D. Alonso, A. J. McKane, and M. Pascual. *J. R. Soc. Interface* **4**, 575 (2007).
 - [10] N. G. van Kampen. *Stochastic Processes in Physics and Chemistry* (Elsevier, Amsterdam, 2007). Third edition.
 - [11] A. J. McKane and T. J. Newman. *Phys. Rev. E* **70**, 041902 (2004).
 - [12] Y. Togashi and K. Kaneko. *Phys. Rev. Lett.* **86**, 2459 (2001).
 - [13] Y. Togashi and K. Kaneko. *J. Phys. Soc. Jpn.* **72**, 62 (2003).
 - [14] D. T. Gillespie. *J. Comput. Phys.* **22**, 403 (1976).
 - [15] M. S. Bartlett. *J. R. Stat. Soc. A* **120**, 48 (1957).
 - [16] R. M. Nisbet and W. S. C. Gurney. *Modelling Fluctuating Populations* (Wiley, New York, 1982).
 - [17] D. T. Gillespie. *J. Chem. Phys.* **81**, 2340 (1977).
 - [18] C. W. Gardiner. *Handbook of Stochastic Methods* (Springer-Verlag, Berlin, 2004). Third edition.
 - [19] H. Risken. *The Fokker-Planck Equation* (Springer-Verlag, Berlin, 1989). Second edition.
 - [20] R. Bellmann. *Introduction to Matrix Analysis* (McGraw-Hill, New York, 1970). Second edition.